

THERMAL QUALIFICATION TESTS OF LONGITUDINAL AMMONIA HEAT PIPES FOR USING IN THERMAL CONTROL SYSTEMS OF SMALL SATELLITES

V. Baturkin, S. Zhuk, D. Olefirenko, A. Rudenko
National Technical University of Ukraine "Kyiv Polytechnic Institute", Kyiv, Ukraine

Abstract

Heat pipes efficiency for space thermal engineering is widely recognized and illustrated. Among majority of heat transfer tasks the heat pipe employment for high precision optical devices' thermal control is interesting and challenging.

Before mounting on a vehicle all heat pipes have to pass through a lot of tests according to corresponding standards and programs.

Main heat pipe qualification tests sequence according to ESA standard is discussed. They include: full performance testing – definition of thermal resistance of heat pipes, maximum heat transfer ability over exploitation temperature range, temperature distribution over the length of heat pipe; start-up capability, priming test; long-life/aging tests, thermal cycling/thermal shocks, burst tests, non-condensable gas definition.

One of discussed questions is choice of thermal sensors' locations at heat pipe tests and the analysis of influence of external associated units on formation of boundary condition in thermal interfaces.

INTRODUCTION

The heat pipes as heat transfer device have a good recommendation for space thermal design. The history of their application in space thermal control has covered more 30 years [1].

Heat pipes can be used as autonomous thermal control systems. Heat pipes service the individual device or group of devices operating independently or in thermal interaction with satellite thermal control system. Practically every system design is specific and used heat pipe type is directly coordinated by device operating requirements.

Performance reliability of heat pipe should be confirmed by qualification tests. Programs of the given tests elaborated in each specific case of heat pipe design particularly depending on scopes and objectives for which the given device is developed.

The main handbook for elaborating the test programs is European Space Agency (ESA)

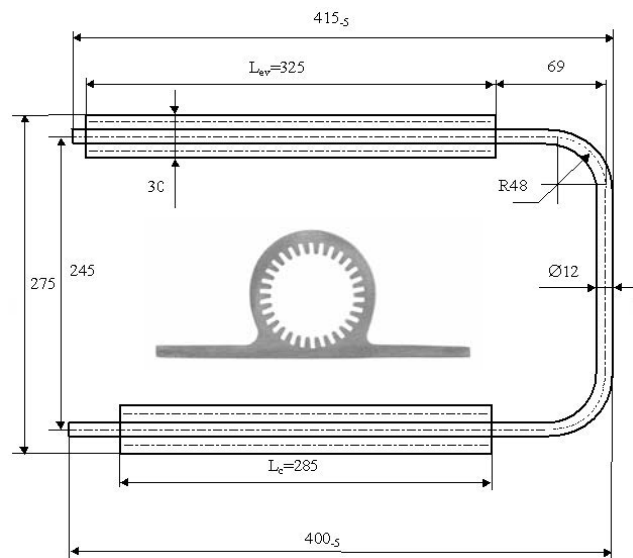


Fig. 1 Diagrammatic drawing of heat pipe and profile of its section in evaporation (condensation) zone (bottom scheme).

requirements. They determine the minimum qualification tests for heat pipes and heat-pipe devices for space applications.

TEST PROGRAM OF HEAT PIPE ELABORATION

Content of heat pipe tests program under BIRD project and test results are presented in this chapter. Heat pipe shell is the round extruded profile with one integral flange made of aluminum alloy AΔ 31. Flanged zones correspond to evaporation zone (325x30x1.2 mm) and condensation zone (285x30x1.2 mm). There is no flange in transport zone. Inside HP shell has capillary structure in the form of 30 longitudinal grooves of rectangular shape (cross section 0.5x1 mm). Ammonia is used as heat carrier. Heat pipes have U-shape geometry by length of working part 951 mm. General view of heat pipe flight modification and its main dimensions are presented in figure 1.

The program and results of heat pipe ground tests under qualification and acceptance program are an additional important questions confirming an ability of heat pipe for space mission tasks. The procedure of the tests is elaborated according to ESA requirement [2] and DLR requirements [3]. The heat pipe test programs for VEGA Project (1984-86), Phobos Project (1986-87), Mars96 have been used as well. The following main tests have been foreseen:

- Inspection and physical measurements
- Proof pressure test - Leak test
- Performance testing
- Burst test
- Random vibration
- Storage simulation test
- Thermal cycles/shock test
- Aging test (long life tests).
- Non-condensable gas definition test.

Among other, the next performance tests are included:

- definition of thermal resistance of heat pipes
- definition of maximum heat transfer ability
- definition of temperature distribution over the length of heat pipe
- definition of priming time of heat pipe after the full dry-out of an evaporation zone (EvZ)
- definition of heat pipe capability to start-up with 80% of maximum heat transport capacity at various vapor temperatures.

In these tests the thermal technical characteristics of heat pipes in a wide range of input heat fluxes (from 5 to 170 W) and constant vapor temperature (t_v) have been checked. Vapor temperature was supported stable at the levels: -50°C, -20°C, 0°C, +20°C, +30°C, +50°C independently of input heat power.

At vapor temperatures -50°C, -20°C the tests were carried out in a vacuum chamber with a nitrogen vaporizer, for $t_v = 0 \div + 50^\circ\text{C}$ the tests have been conducted in air medium with force liquid cooling of condenser zone.

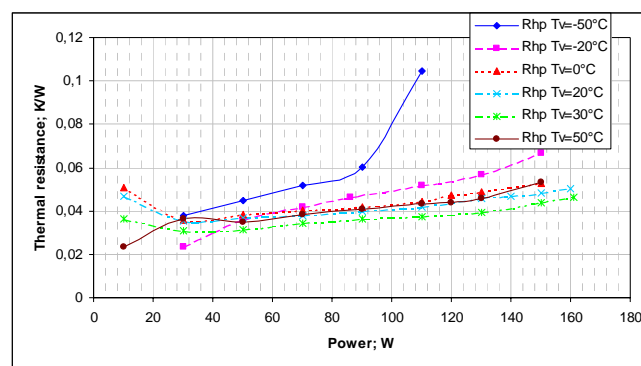


Fig. 2 Dependence of thermal resistance of heat pipe on input heat flux and temperature level.

Dependencies of thermal resistance R_{hp} for heat pipes of configuration shown in figure 1 on input power for various vapor temperatures are presented in figure 2. Thermal resistance was defined on base of averaged temperature of evaporator zone \bar{T}_{ev} and condenser zone \bar{T}_{con} and net heat power transported Q

$$R_{hp} = (\bar{T}_{ev} - \bar{T}_{con}) / Q \quad (1)$$

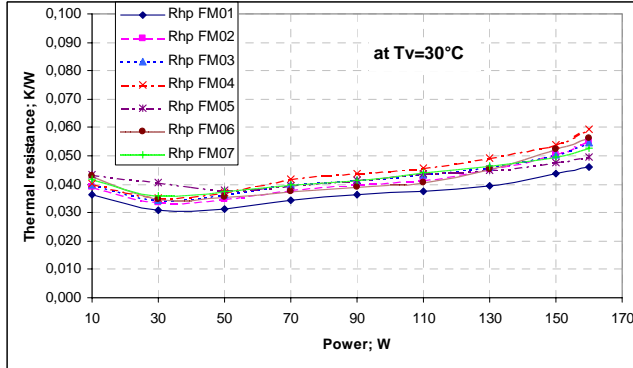


Fig. 3 Dependence of heat pipe thermal resistance on input heat flux for heat pipes of flight model series.

As one can see from graphs, practically all dependencies have a tendency to increase. The cause of increasing the thermal resistance with input power rise deals with decreasing heat exchange efficiency in condensation zone. The last changing occurs due to the liquid film thickness rise in this zone. Liquid condensate may flow down towards bottom part of inner surface and may broaden the boundary of streamlet.

With rising of input power, the characteristic curve approaches to critical zone of heat pipe operation where a sudden change of thermal resistance occurs due to overheating of end point of heat pipe evaporation zone. This phenomenon deals with dry-out of some upper grooves.

For heat pipes of one manufacture series, experimental dependencies $R_{hp}=f(Q)$ (fig. 3) have the similar behavior, and the value dispersion of R_{hp} for the same value of power transferred is no more than 0.01 K/W. Such behavior and the values' dispersion are observed on boundary temperatures -50 and $+50$ °C as well.

Quantitative change of the value of heat exchange coefficients in HP evaporator depending on vapor temperature and input power is presented in figure 4. Heat-transfer coefficients in evaporation α_{ev} and condensation α_{con} zones of HP are defined as:

$$\alpha_{ev} = \frac{Q}{(\bar{T}_{ev} - \bar{T}_v) \cdot F_{ev}}, \quad (2)$$

$$\alpha_{con} = \frac{Q}{(\bar{T}_v - \bar{T}_{con}) \cdot F_{con}}, \quad (3)$$

where \bar{T}_v , [°C] - average temperature of heat pipe vapor measured as shell temperature in transport (adiabatic) zone; $F_{ev/con} = \pi \cdot d_{in}^2 \cdot L_{ev/con}$, [m] – assumed heat-transfer surface, where d_{in} - inner diameter of heat pipe shell (\varnothing 8 mm), $L_{ev/con}$ - length of evaporation zone or condenser

The behavior of obtained curves shows relatively small dispersion of heat exchange coefficients depending on input power and a considerable fluctuation of their values from vapor temperature. Such interrelation can be explained that the intensity of evolution of evaporation process is a defining factor. The peculiarities of this process should be further studied in details.

Heat exchange coefficients in condensation zone (ConZ) have another character. This dependence is presented in figure 5. Within the limits of error there is possibility to assume the low level of influence of temperature on value of heat exchange coefficient in condenser.

Definition of maximum heat transport rate of HP (Q_{max}) is realized by two techniques, recommended in [2] and [4]. The combined dependence $Q_{max}=f(t)$ is presented in figure 6. Typical rise and plateauing of the curve at approaching the values of Q_{max} to positive vapor temperatures corresponds with conditions when evaporation intensity in EvZ of heat pipe reaches the maximum and becomes practically constant within vapor temperatures $+15 \div 50^{\circ}\text{C}$. Character of this curve corresponds with data [1].

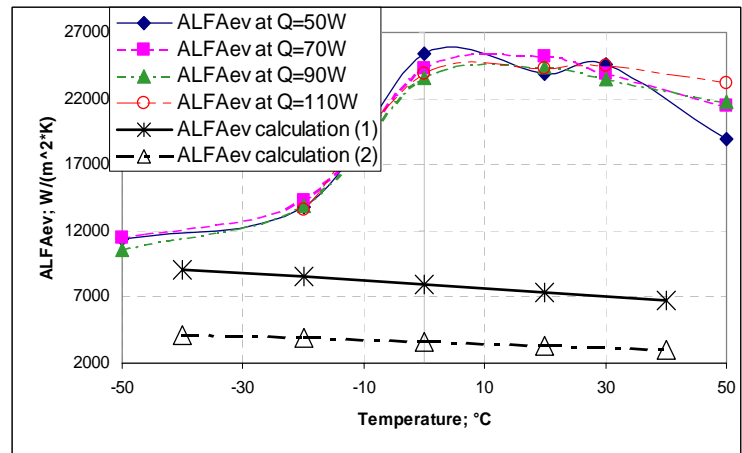


Fig. 4 Dependence of experimental heat exchange coefficients (ALFAev) and calculated ones in evaporation zone on vapor temperature for different input powers.

Calculation was made by Kamotani's (1) and Chi's (2) formulas

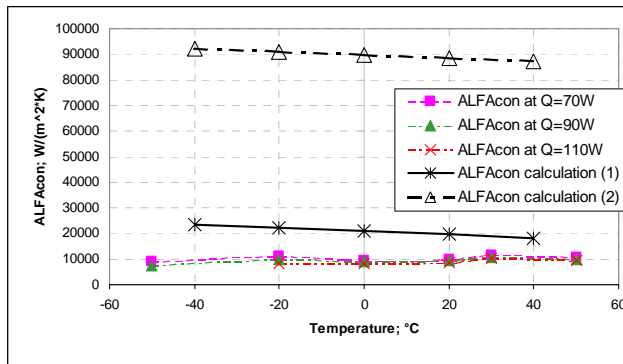


Fig. 5 Dependence of heat exchange coefficients (ALFAcon) and calculated ones in condensation zone on vapor temperature for different input powers.

Calculation was made by Kamotani's (1) and Chi's (2) formulas.

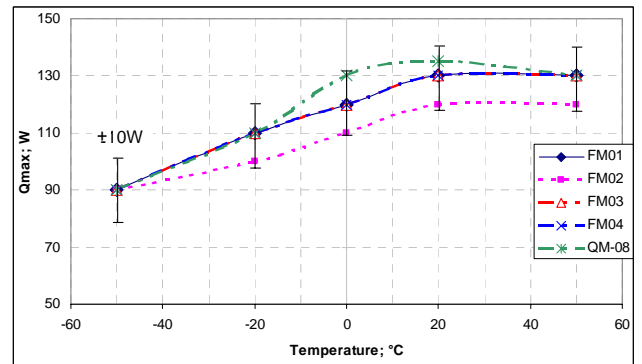


Fig. 6 Dependence of maximum heat transport rate on vapor temperature for flight models of heat pipes. Horizontal position. Vertical bars – possible errors of heat ability measurement.

One of extended indicators specifying heat pipe performance is temperature distribution along its length.

In figure 7 this characteristic curve is shown at extreme values of vapor temperature -50°C and $+50^{\circ}\text{C}$ and the same heat flux. In transport zone both curves do not differ qualitatively, however with moving from transport zone to ends of heat pipe the difference becomes more visible. So for the conditions $t_v = +50^{\circ}\text{C}$ the temperature drop along the whole heat pipe is about 4.4°C , and at $t_v = -50^{\circ}\text{C}$ it equals 6.2°C (at 90 W power).

Difference in evaporator deals with the beginning of overheating at $t_v = -50^\circ\text{C}$ (see figure 10 as well). Increase in temperature of the end point of EvZ is connected with partial drainage of this area. This occurs by reason of underfilling the grooves by a heat carrier because of decrease in its volume that takes place at temperature reducing and possible “breaking” of a liquid phase by vapor flow, the velocity of which at low pressure increases considerably and reaches 30 m/sec [5].

Distinctions in condenser temperature profile associate with (a) other type of cooling equipment used at $t_v = -50^\circ\text{C}$ and $+50^\circ\text{C}$ correspondingly and (b) probable influence of non-condensable gas plug at lower temperatures. At lower temperatures and pressures the gas block expands more and influences on thermocouple indications.

Important indicator confirming the correctness of heat carrier amount in heat pipe is the priming time. During this time filling of the capillary structure with liquid occurs after its complete drainage. Imitation of this phenomenon on heat pipe having stationary state of power transfer equal $0.8 \cdot Q_{\max}$ was carried out by sudden overturning from horizontal to vertical position (EvZ is up) and returning to initial position. Graph dependencies by means of which a priming time was defined are presented in figure 8 (reading makes from 0 sec that is overturning a heat pipe from horizontal to vertical position). As result of this manipulation the heat carrier merges in transportation zone that leads to active temperature increase in the evaporation zone end and initial parts.

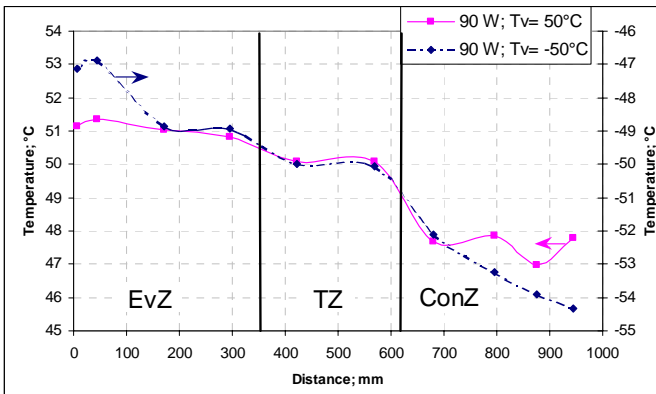


Fig. 7 Temperature distribution along heat pipe for various t_v and input power 90W.

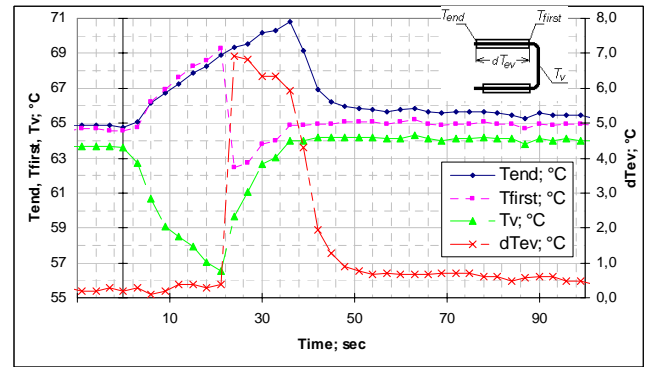


Fig. 8 Definition of priming time. T_{end} - the temperature dependence in the end point of evaporation zone; T_{first} - the temperature dependence in the initial point of evaporation zone; T_v - vapor temperature and dT_{ev} - the temperature drop of heat pipe over evaporation zone length.

On heat pipe overturning to horizontal position the initial point of EvZ fills up with liquid again, its temperature falls, a temperature difference along EvZ abruptly increases. This moment is considered to be the beginning of priming. Priming time is defined as a finish of reducing of temperature drop in EvZ (dT_{ev} , figure 8) and its reaching the constant level. For the given case, a priming time equals 30 sec.

In addition to the main heat exchange characteristics of heat pipes (thermal resistance, heat exchange coefficients, maximum heat transport rate) stability and recurrence of measurement values at influence of gravity and imitation of start conditions also were estimated in tests. Routinely variation in time of long life characteristics of HP was studied as well. Ratio of current thermal resistance to thermal resistance at the beginning of operation obtained during the long life tests is presented in figure 9.

Tests were carried out at constant vapor temperature (about $+50^{\circ}\text{C}$, fluctuation was no more $\pm 5^{\circ}\text{C}$) and transferred heat flux - $90 \pm 2 \text{ W}$. The values of thermal resistance of all heat pipes (4 units) are stable enough in time (no less than 10000 hours). This fact characterizes positively the quality of their fabrication and long life capacity for work. Certain individualization of value of R_{hp} for each HP can be explained by the difference of values of their charge with the heat carrier. Data scatter in these tests is no more than $\pm 10\%$ that is within ordinary error of experiment.

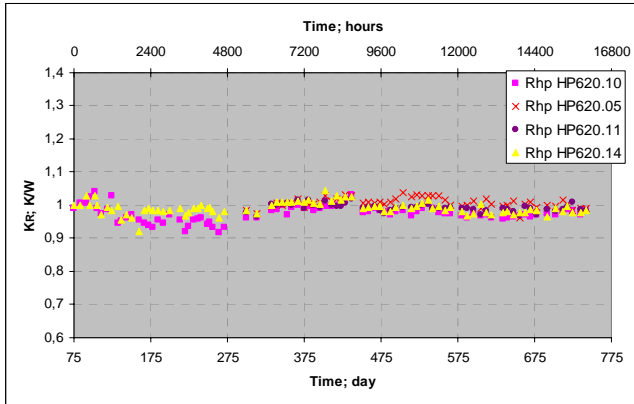


Fig. 9 Results of measurements of thermal resistance of heat pipes in time. K_R – ratio of current thermal resistance to thermal resistance in the beginning of working.

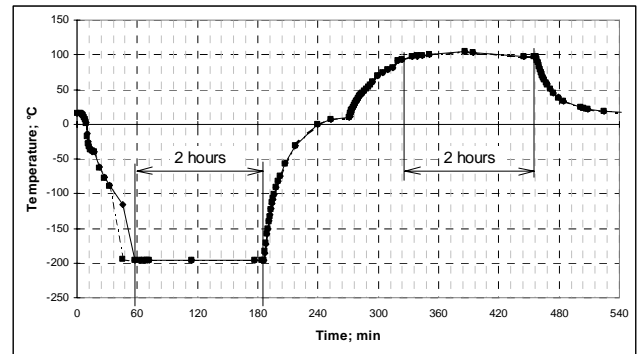


Fig. 10 Changing temperatures during storage simulation test.

Heat pipe capability to maintain own tightness and to continue normal operation after fluent and sudden working temperature changes from low to high levels and vice versa has a great importance. For checking this capability the thermal cycles/thermal shock tests and storage simulation tests were carried out. In thermal shocks tests a heat pipe was subjected to multifold influence of low (-60°C) and high ($+80^{\circ}\text{C}$) temperatures. Temperature change from one to another is no more than 2 min. Depending on the heat pipes status (thermal, qualification or flight model) they are subjected to 16 (for flight model) ÷ 300 (for qualification model) time cycles. Tightness of heat pipes before and after the tests has been checked by two chemical developers of ammonia. The first one named "Color-3" looks as flexible 0.3 mm thick tape (Elaboration of Institute of Physical Chemistry of National Academy of Science of Ukraine). The second one is the spray ADP-19 by American Gas&Chemical Co.



Fig. 11 Three samples of burst heat pipes.

Storage simulation tests are intended for checking a capability of heat pipe to stay a long time at low and high temperatures. Lowest test temperature was provided with boiling nitrogen at atmosphere pressure (-196°C), and maximal temperature – by means of a drying box in the working volume in which air temperature level $+100^{\circ}\text{C}$ was maintained. Heat pipe was subjected to 5-time cycles.

Maintenance of thermal technical characteristics of heat pipes during whole flight of space vehicle depends on many factors, one of which is strength and shell tightness. Each elementary unit of vehicle equipment should have a certain margin of safety needed for reliable and trouble-free operation.

Towards this end the tests of strength characteristics of heat pipe are carried out.

For decision of the given problem an experimental bench was created and the procedure of calculation of stresses appeared in heat pipe at its operation both in optimum and in emergency (shell bursting) situation was developed.

As calculations have showed on developed procedure, the stress appeared in heat pipe shell at its operation in the optimum situation ($t_{work}^{max} = 60^{\circ}C$, $P_{NH_3} = 26.127 \cdot 10^5 Pa$) in 2.03...5.4 times less than a permissible stress. So, the strength of heat pipe shell is ensured in this case.

The pressure at which the heat pipe depressurization occurs is defined by an average temperature of the heat pipe wall at burst moment.

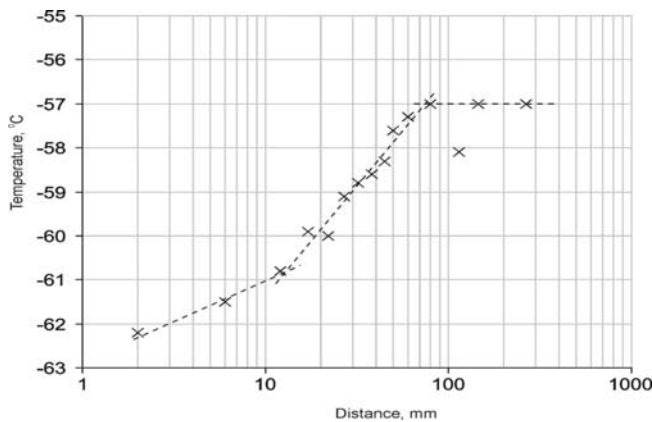


Fig. 12 Distribution of heat pipe shell temperature in gas plug area.

Visual inspection of heat pipes and places of their destruction (figure 11) shows that the burst occurs in different shell sections independently of presence or absence of fins and curving in this place. This fact can be explained that the depressurization occurs where non-uniformity of heat pipe shell thickness takes place.

Tests on definition of non-condensable gas (NCG), which is gassing inside the heat pipe in process of heat pipe function, were included in the qualification test program.

The tests were carried out on special bench which has two thermal insulated compartments (upper and lower) into which condensation and

evaporation zones of each test heat pipe were mounted correspondingly. The temperature test range was – 10... –57°C. Taking into account that NCG plug is situated closer to the condensation zone end the measuring of temperature field in this part of heat pipe was mainly attended. On results of measurement for each heat pipe the diagrams of temperature measurement of heat pipe shell in the zone of NCG plug location are plotted (fig. 12).

The plug length is considered to be a part on which a slump of temperature occurs because of NCG presence which prevents the condensation of heat carrier vapor on the heat pipe wall.

At calculation of NCG quantity it was assumed:

- main component of NCG is hydrogen;
- temperature of NCG plug is closer to heat pipe temperature wall because of small geometrical size and high thermal conductivity of heat pipe shell material;
- temperature of saturated vapor of ammonia is equal to the heat pipe wall temperature in the adiabatic (transportation) zone.

NCG volume and NCG quantity are calculated after definition of plug size for each temperature regime of test heat pipe.

TEMPERATURE MEASUREMENT PECULIARITIES

As was noticed above the heat pipes with one-sided flange shells were used (figure 1). This means non-uniform heat input in cross-section and essential temperature gradient in shell [1]. On stage of heat pipe elaboration and design as draft assumption the uniform temperature distribution over perimeter of heat pipe section was accepted. However further experimental investigations have shown the essential temperature non-uniformity. Depending on the position of thermal sensor's mounting over the perimeter one can obtain the considerable difference in the temperatures characterizing the heat pipe inner processes. For temperature measurement in evaporation and condensation zones the places for sensor mounting were selected at the crossing point of HP cylinder part and the flange (point A, figure 13). Sensors in transport zone were attached to the upper generatrix of the shell.

The experimentally defined temperature distribution in evaporator zone over an unfold section for various input powers is presented in figure 13.

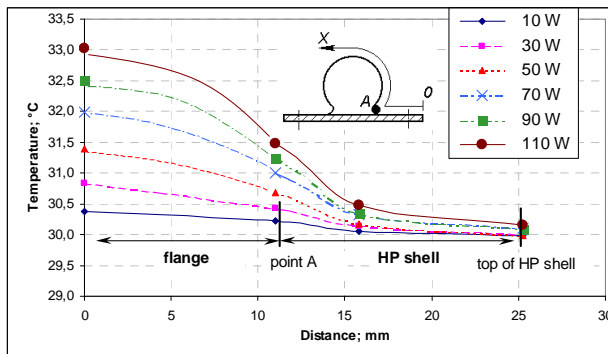


Fig. 13 Temperature variation in shell along reaming surface of heat pipe cross section.

Investigations were carried out for two schemes of heat input and removal: directions of gravity and heat flux are opposite; directions of gravity and heat flux are coincident. For each case the heat exchange coefficients on the base of average integral temperature α_{av} and the heat exchange coefficients on base of the temperature of sensor at point A were calculated.

By the obtained heat exchange coefficients one can calculate the re-calculation coefficient K :

$$K = \alpha_{ev} / \alpha_A \quad (4)$$

Dependence of the re-calculation coefficients on input power is shown in figure 14. Re-calculation coefficients are approximately constant for each power value and have a tendency of convergence to 2.

Absolute difference of values calculated on the base of the average integral temperature is more twice than ones calculated on the base of the point A temperature. This conclusion is valid for certain design of heat pipe cross section.

At non-uniform distribution of temperatures over the section perimeter, the definition of heat pipe thermal characteristics based on the shell average integral temperature is seen to be rational. However, carrying out a great number of heat pipe tests under qualification, acceptance program with usage of the average integral temperature is very time-consuming. So comparison and analysis of results obtained on base of the average integral temperature and on base of the temperature of one sensor located in point A were carried out.

For defining the average integral temperature, three temperature sensors were mounted on HP

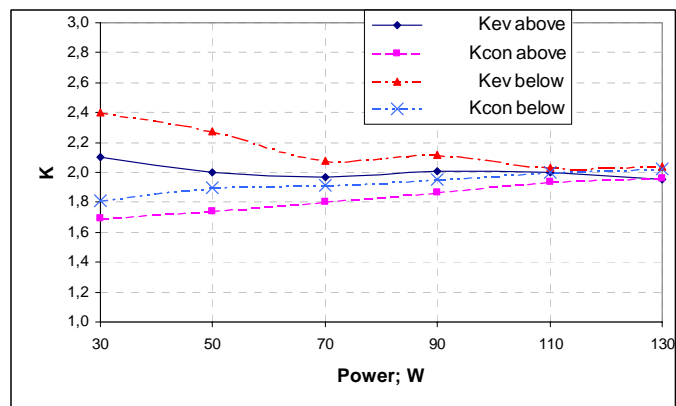


Fig. 14. Dependence of re-calculation coefficient on input power. Kev above – heat input from above, Kcon above – heat removal from above, Kev below – heat input from below, Kcon below – heat removal from below

The interconnection between the location of temperature sensor at non uniform boundary conditions and the value of intensity of inside heat exchange is probably the reason of incompatibility of experimental results obtained in different research Labs, every of which uses own methodic temperature sensors location and own algorithm of data processing and interpretation.

Contact

Exchange of information in related areas can be realized via emails: baturkin@carrier.kiev.ua.

References

1. B & K Engineering, Inc. Brennan P., Kroliczek E. Heat Pipe Design Handbook. Contract No NAS5-23406, June 1979.
2. Qualification requirements to heat pipes. ESA PSS-49 (TST-01). Issue 2, March 1983
3. Environmental test requirements for spacecraft bus components. AF-BIRD-6100-WS/006, 1. Issue dated 13.01.97
4. Semena M. Gershuny A., Zaripov V. Heat pipes with metal Felt Capillary Structures.- Kyiv, Publishing house "Vyscha skola", 1984, 215 p.
5. Heat pipes/edited by E. Shpilrin. Moscow, - Mir, 1972